



Simplify your imaging workflows

**Make research imaging workflows accessible, traceable,
and secure with Athena Software for Core Imaging Facilities.**

Thermo Scientific™ Athena Software is a premium imaging data management platform designed for core imaging facilities that support materials science research.

Athena Software ensures traceability of images, metadata, and experimental workflows through an intuitive and collaborative web interface.

Find out more at thermofisher.com/athena

ThermoFisher
SCIENTIFIC

Elastic-Connection and Soft-Contact Triboelectric Nanogenerator with Superior Durability and Efficiency

Zhiming Lin, Binbin Zhang, Yiyuan Xie, Zhiyi Wu, Jin Yang, and Zhong Lin Wang*

Triboelectric nanogenerator (TENG) has received tremendous attention in ambient energy harvesting, especially for ocean wave energy. However, the technology is generally challenged to obtain excellent durability and high efficiency simultaneously, which primarily overshadows their further industrial-scale applications. Here, a dual-mode and frequency multiplied TENG with ultrahigh durability and efficiency for ultralow frequency mechanical energy harvesting via the elastic connection and soft contact design is proposed. By introducing the spring and flexible dielectric fluff to the novel pendulum-like structural design, the surface triboelectric charges of TENG are replenished in soft contact mode under the intermittent mechanical excitation, while the robustness and durability are enhanced in non-contact working mode. The fabricated TENG results in a continuous electrical output for 65 s by one stimulus with a high energy conversion efficiency, as well as negligible change of output performance after a total of 2 000 000 cycles. Moreover, integrated with the power management circuit, the TENG array is demonstrated to drive the electronics by effectively harvesting wind and water wave energy as a sustainable energy source. This work paves a new pathway to enhance the robustness, durability, and efficiency of the TENG that resolves the bottleneck of its practical applications and industrialization.

covering more than 70% of the earth's surface contains abundant resources due to the advantages of wide distribution and sufficient availability, and ocean waves are one of the most promising renewable clean energy resources for large-scope scavenging and utilization.^[4–7] Therefore, harvesting the wave energy to power the sensing nodes has been considered an ideal way for the remote and self-powered sensing monitoring system in the ocean. Extensive research efforts have been dedicated to harvest wave energy based on the piezoelectric, electromagnetic, and triboelectric effect.^[8–11] Among them, triboelectric nanogenerator (TENG, also named as Wang generator) has been demonstrated as a prospective technology to extract mechanical energy into electricity as a green, self-sufficient, sustained energy-supplying source^[12–17] and the self-powered sensor for the sensor network systems.^[18–24]


Tracing the fundamental from Maxwell's displacement current, TENG based on the coupling of triboelectrification and electrostatic induction, features high output voltage, high efficiency, cost-effective, versatile choices of materials, and environmental friendliness due to its distinct mechanism.^[25–29] Since its invention in 2012, enormous efforts including materials development, structure, and circuit design have been paid for large-scale wave energy harvesting to archive the blue energy dream.^[30–33] However, the TENG still suffers from weak durability, low efficiency, and short operation time, which greatly limits its long-term practical applications and industrialization.

1. Introduction

The rapid growth of the Internet of things (IoT), mobile internet technology, and sensor network systems has increased the demand for distributing and mobile operated sensing nodes to achieve in situ and real-time information sensing.^[1–3] Such ubiquitous sensors, especially distributed in the ocean stimulate the requirements for a sustainable, maintenance-free, and self-sufficient power source. As is known to all, the ocean

Dr. Z. Lin, Prof. Y. Xie
School of Electronics and Information Engineering
Southwest University
Chongqing 400715, China

Dr. B. Zhang
Key Laboratory of Advanced Technologies of Materials
(Ministry of Education)
School of Materials Science and Engineering
Southwest Jiaotong University
Chengdu 610031, China

 The ORCID identification number(s) for the author(s) of this article can be found under <https://doi.org/10.1002/adfm.202105237>.

DOI: 10.1002/adfm.202105237

Prof. Z. Wu, Prof. Z. L. Wang
Beijing Institute of Nanoenergy and Nanosystems
Chinese Academy of Sciences
Beijing 100083, China

Prof. J. Yang
Key Laboratory of Optoelectronic Technology & Systems
(Ministry of Education)
Department of Optoelectronic Engineering
Chongqing University
Chongqing 400044, China

Prof. Z. L. Wang
School of Materials Science and Engineering
Georgia Institute of Technology
Atlanta, GA 30332-0245, USA
E-mail: zhong.wang@mse.gatech.edu

Our previous work suggested an effective solution to improve the durability and lifetime of the TENG by introducing a spring structure operating in non-contact mode and replenishing the surface charge intermittently.^[34] Additionally, the frequency-multiplied strategy was proposed in our recent work to boost the energy conversion efficiency of TENG directly, which shows great potential in ultra-low frequency wave energy harvesting.^[35] Given all this, the development of TENG that works in non-contact mode with frequency-multiplied feature would simultaneously improve the durability and energy conversion efficiency of which.

Herein, an elastic-connection and soft-contact TENG (ES-TENG) with simultaneous boosted durability and efficiency is proposed for the first time, which performs well in ultra-low frequency water wave energy harvesting. In detail, a pendulum-like structure was designed as the sensitive component for external mechanical excitation, leading to an air gap between the triboelectric layers. As a result, the ES-TENG can work in the non-contact mode without any frictional resistance, thereby enhancing the robustness and durability of the proposed device. Moreover, the elastic connection and soft contact were achieved by introducing the spring and flexible dielectric fluff in the pendulum, therefore the surface triboelectric charges can be replenished by the intermittent mechanical excitation, resulting in high efficiency with multiplied frequency. The output characteristics of the ES-TENG device was systematically investigated by various mechanical trigger times and structure parameter and the durability and robustness of the device were detailed revealed from the view of output performance and materials abrasion. Compared to the rigid-connection TENG, the output voltage, and current, of the ES-TENG were increased to 741%, and 822%, respectively. Besides, the ES-TENG presented high energy conversion efficiency of 29.7% and excellent durability after continuously operating for 2000000 cycles. Finally, the ability of integrated ES-TENG networks for harvesting wave energy as sustainable power sources for self-powered environment monitoring systems was successfully illustrated. The ES-TENG with excellent durability and high efficiency presents a fundamental strategy for sustaining wave energy harvesting research and promotes its industrialization and practical applications in IoTs.

2. Results and Discussion

The idea map of future ES-TENG networks to harvest the wave energy for powering sensing nodes to realize the self-powered monitoring system in the ocean is proposed in **Figure 1a**. The structure of the single device is illustrated in **Figure 1b** that is an integration of two major parts, namely, the cambered triboelectric layer and pendulum-like sensitive component. The cambered polytetrafluoroethylene (PTFE) film is mounted on the spherical shell as the triboelectric layer, under which an internal circular and an external ring electrodes are deposited on the acrylic substrate. As for the pendulum-like sensitive component, the elastic-connection part is composed of a spring and two rigid rods and the flexible dielectric fluff acts as the soft-contact and freestanding triboelectric layer, as the real component shown in **Figure 1c**. The pendulum is connected to the

outer acrylic spherical shell by a cotton thread, resulting in an air gap between the triboelectric layers, which guarantees the extremely sensitive oscillation and reduces the materials abrasion resulted from the external mechanical excitation even a small disturbance. Furthermore, to enhance the triboelectric effect, the nanowire structure is modified on the PTFE surface to improve the effective contact area between the triboelectric pairs, as demonstrated in **Figure 1d**. The photograph of the as-fabricated ES-TENG network is exhibited in **Figure 1e**.

The fundamental working principle of the designed ES-TENG relies on the unique coupling of triboelectrification in contact-separation mode and electrostatic induction in free-standing mode, as schematically demonstrated in **Figure 1f**. In detail, at the initial state (i), there exist no original charges on the surfaces of the triboelectric layers due to the air gap between the two layers. Once an external mechanical excitation like a water wave is applied to the ES-TENG, the spring will be stretched because of the inertial force in the pendulum, resulting in the contact between the triboelectric pair naturally, as shown in stage (ii). The electrons transfer from the flexible dielectric fluff to the surface of PTFE film, thereby generating an equal amount of positive and negative triboelectric charges on the two surfaces, respectively, due to the difference of the electron affinity. Subsequently, the spring will restore to the original state depending on its restoring force, leading to the separation of the charged triboelectric layers, and the triboelectric charges on the triboelectric surfaces will be saturated after several excitations. This is the charge pumping process with the assisted spring for triboelectrification.

As stated above, the pendulum-like component swings without frictional resistance periodically at free-standing mode owing to external disturbance such as water waves. At stage iii, while the pendulum-like component is driven to swing leftward from the balanced state, an electrical potential difference is built and then drives the electrons flowing from the circular electrode to the ring electrode through the external load. Then, the electrons flow back from the ring electrode to the circular electrode to eliminate the potential difference as the pendulum-like component swings rightward, generating a reverse current in the circuit and forming a complete cycle of the electricity generation process. When the pendulum keeps swinging rightward, the same electrons flowing process will be happened as similar to swings leftward above, as shown in state iv. There is little frictional resistance in the swing process, which is contributed to the periodically multiple swings at ultra-low frequency external excitation, resulting in multiplied output performance. Moreover, such motion behavior reduces the triboelectric material abrasion, benefiting the durability and long-term work of the ES-TENG.

To understand the fundamental output characteristics of the ES-TENG, it is tested with a programmable linear motor that can simulate the agitation of water waves. The electrical output including the open-circuit voltage, short-circuit current, and short-circuit transferred charges are evaluated systematically. **Figure 2a** shows the open-circuit voltage of the proposed ES-TENG by an external mechanical agitation. It indicates that the electrical output can last over 65 s with the continuous swing due to little frictional resistance between triboelectric layers, showing excellent frequency-multiplied performance.

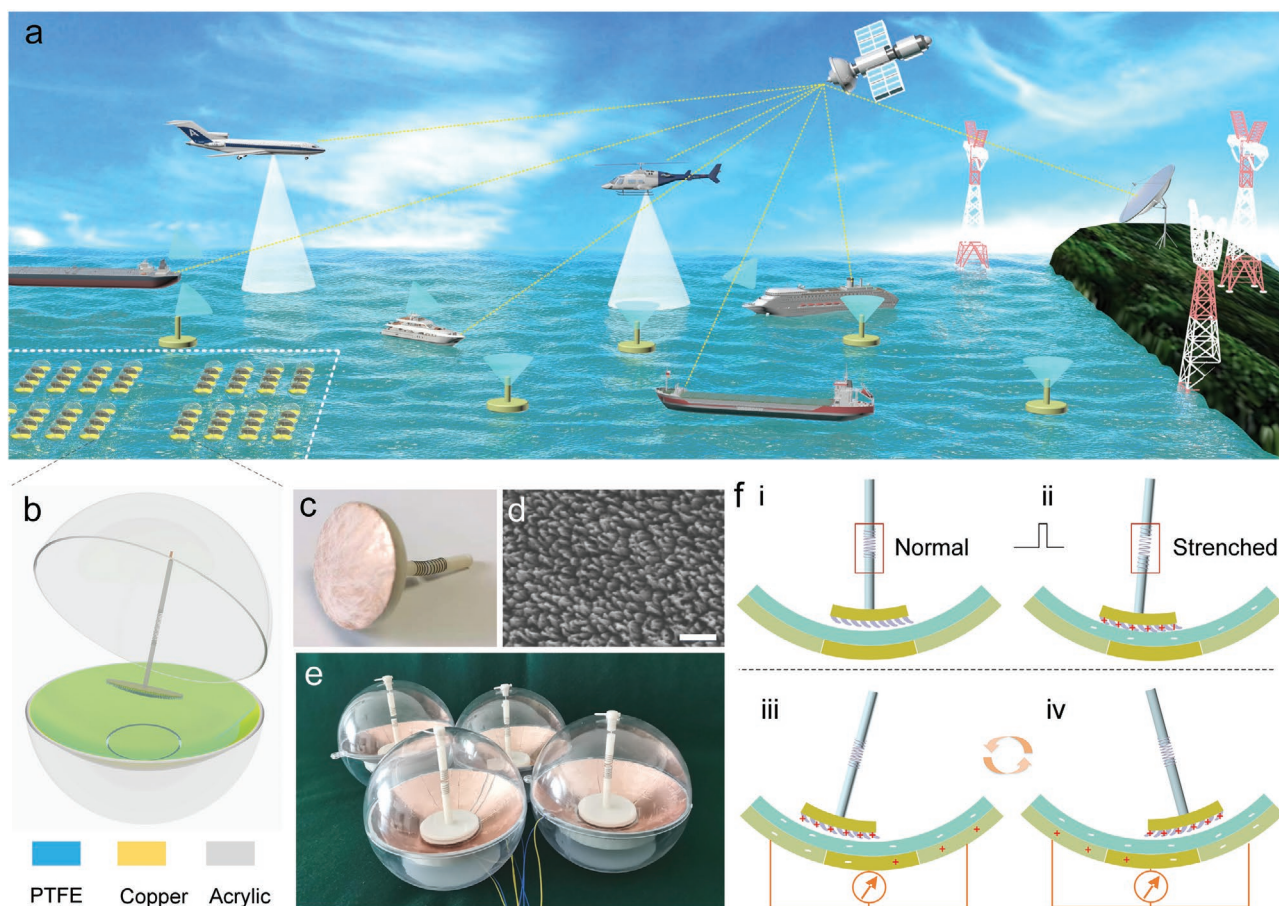


Figure 1. Structural design and working principle of the proposed ES-TENG. a) Schematic diagram of the ES-TENG networks for harvesting the wave energy to realize the self-powered monitoring system in the ocean. b) Schematic illustration of the ES-TENG composed of cambered triboelectric layer and pendulum-like component. c) Photograph of the fabricated pendulum-like component. d) SEM images of the etched PTFE film. Scale bar, 500 nm. e) Photograph of the fabricated ES-TENGs. f) Working principle of the proposed ES-TENG at i) initial non-charged state and ii–iv) charged state under the external mechanical excitation.

The short-circuit current and transferred charges show a similar trend with the open-circuit voltage, as demonstrated in Figure 2b,c. More important, the attenuation rate of the open-circuit voltage drops by 10% after 7.2 s due to the effect of air friction, which means that the proposed ES-TENG is capable of generating frequency-multiplied output with high electrical performance even stimulated by 0.138 Hz external agitation. Such output characteristics and working frequency are perfectly suitable for ultra-low frequency wave energy harvesting. Besides, Table S1, Supporting Information, also indicates that the attenuation rates of output performance are consistent in different excitation directions, which is contributed to the spatially symmetric structural design of the pendulum model. To systematically identify the influence of the spring and flexible dielectric fluff on the output performance, various pendulum-like components are carried out to compare the electrical outputs at the same simulation condition, as demonstrated in Figure 2d. Here, we employed the pendulum-like components without the spring and fluff (Device 1), without the fluff (Device 2), and with the spring and fluff (our Device, named Device 3) for these comparison experiments. Figure 2e depicts that the open-circuit voltage and short-circuit current of Device 2 are

larger than that of Device 1, indicating the spring is beneficial to the triboelectrification for charge accumulation. Moreover, the output amplitudes of Device 3 are larger than that of Device 2 distinctly, rendering that the fluff contributes to increasing the effective frictional area for much more transferred charges. The short-circuit transferred charges result of the three devices also verifies such principle, as illustrated in Figure 2f. Device 1 has an output voltage of 10.2 V, while Device 3 produces an output voltage of 75.6 V, an increase of 641%. Meanwhile, the short-circuit current increases from 0.09 to 0.74 μA , growing by 722%. To further comprehensively investigate the charge pumping process of the ES-TENG, the linear motor is employed to provide continuous periodic triggers for the observations of output amplitude and transferred charge quantity, as shown in Figure 2g,h. The amplitude of open-circuit voltage increases from 10 to 76 V with the growth of continuous trigger times from 1 to 7 and then slows down, the sloping trend of short-circuit current is also consistent with the voltage, as demonstrated in Figure S1, Supporting Information. Figure 2h depicts the short-circuit transferred charge quantity for the ES-TENG by the continuous triggers, it is observed that the charge quantity increases linearly at the early stage, and then stables at ≈ 27 nC

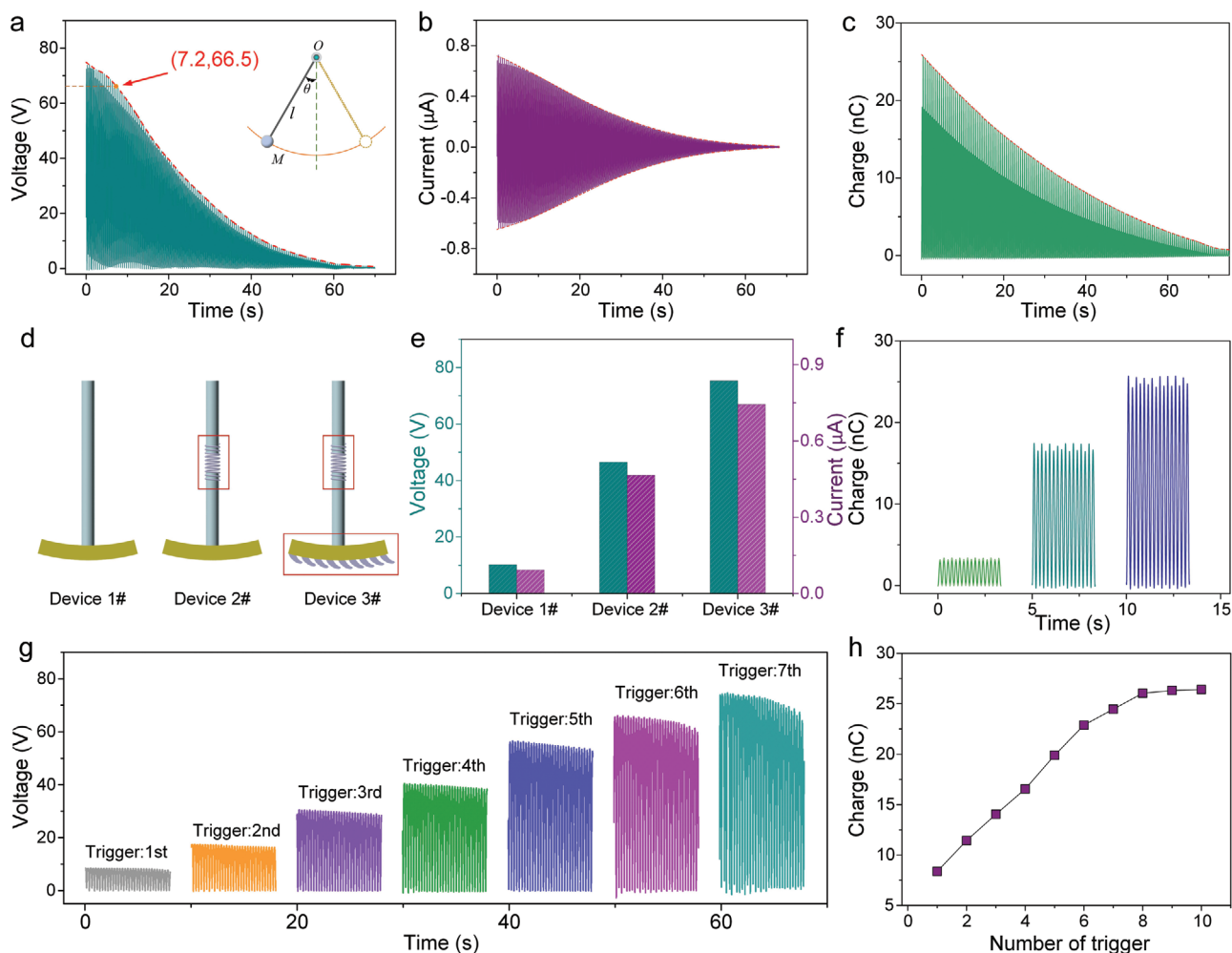


Figure 2. Electric performances of the ES-TENG. a) Open-circuit voltage, b) short-circuit current, and c) short-circuit transferred charge of the proposed ES-TENG under an external stimulus. d) Schematic diagram of various pendulum-like components. e) Open-circuit voltage, short-circuit current, and f) short-circuit transferred charge for three different pendulum-like components. The amplitudes of g) the open-circuit voltage, and h) short-circuit transferred charge quantity under the continuous stimulus.

after eight triggers. Hence, the availability of the spring-assisted pendulum-like structure for triboelectrification is successfully substantiated by the above experimental results.

The robustness and durability of the TENG are considered as the paramount characteristics for long-term effective energy harvesting in practice, as shown in **Figure 3a–c**, they are investigated through enormous period experiments. As shown in **Figure 3a**, the open-circuit voltage of the ES-TENG shows negligible drops after continuous operation of 60 min. Moreover, **Figure 3b** and **Figure S2**, Supporting Information, displayed little decline of the open-circuit voltage (Attenuation: 2.76%, shown in **Figure S3**, Supporting Information) and short-circuit current for long-term continuous operation even after a total of 2000000 cycles, convincing superior stability and robustness of the as-fabricated device, convincing superior stability and robustness of the as-fabricated device. Furthermore, the surface material abrasion of the PTFE film is captured by scanning electron microscopy (SEM), as demonstrated in **Figure 3c**. It serves to show that nanowire structures on the surface of PTFE film preserve well and no obvious damage and abrasion for the

triboelectric material, rendering the excellent durability of the ES-TENG for long-term work. Such superior stable and durable features of the ES-TENG are mainly attributed to the innovative design of spring-assisted pendulum-like structure with air gap at non-contact working mode. Additionally, external load resistors are used to characterize the electrical outputs of the ES-TENG for energy harvesting capacity, and the peak current–resistance and peak power–resistance relationships are shown in **Figure 3d**. As the load resistance increases, the peak value of the current decreases due to the Ohmic loss, and the maximum peak power of 28 μW is achieved at a matched load resistance of 100 $\text{M}\Omega$, which can be calculated by $P = I^2R$. And the charging performance of the ES-TENG for different capacitors is also explored, as depicted in **Figure S4**, Supporting Information. Charged by the ES-TENG, the voltage of capacitors with a value of 3.3 and 10 μF can reach up to 3.8 and 1.5 V in 30 s. Moreover, to investigate the energy conversion efficiency of ES-TENG for just one triggering, the generated electrical energy obtained at matched load resistance can be evaluated by $E = \int I(t)^2 R dt$, where $I(t)$ is the instantaneous current across the

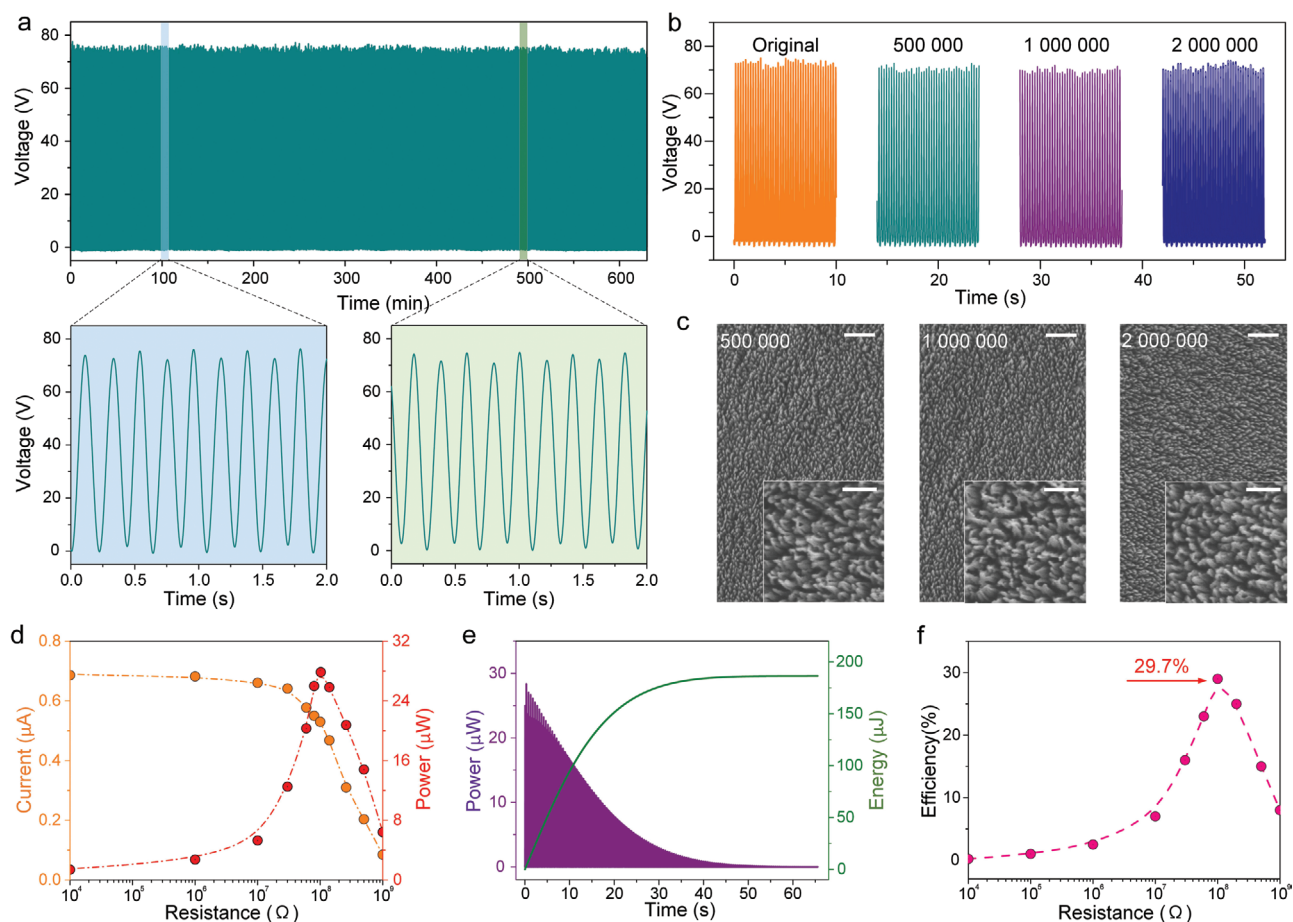


Figure 3. Long-term durability test and output power of the ES-TENG. a,b) The durability test of the TENG operating over a) 60 min and b) various cycles. c) Comparison of the surface morphology of the PTFE film over various cycles. Scale bar, 1 μm . Inserted scale bar, 500 nm. d) Output current and power under different resistances. e) Output power and converted energy for a stimulus. f) The energy-to-electric energy conversion efficiency at different load resistances.

resistor at the time t , and R is the load resistance. Figure 3e shows the instantaneous output power and generated electrical energy, which increases continuously over time and achieves the value of 186 μJ , ultimately. Here, we calculate the vibration energy-to-electric energy conversion efficiency through the generated electrical energy after one stimulus divided by the acquired vibrational energy induced by an external trigger. The vibrational energy can be evaluated by the difference of gravitational potential energy between the highest center of gravity and that at the final state for one stimulus, as schematically demonstrated in Figure S5, Supporting Information. Hence, the efficiency can be expressed as:

$$\eta = \frac{E_{\text{out}}}{E_{\text{in}}} = \frac{\int I(t)^2 R dt}{mg\Delta h} \quad (1)$$

where m donates the mass of the swing component, g is the gravitational acceleration, and Δh refers to the height difference between the center of gravity at the highest and final states, we obtained the two values by capturing the photographs for the two states from a slow-motion video of the ES-TENG

movement. Figure 3f indicates that the maximum efficiency of 29.7% achieved at the matched resistance of 100 $\text{M}\Omega$, indicating much outstanding efficiency than the previous works as schematically illustrated in Table S2, Supporting Information. The detailed calculation method for the energy conversion efficiency is clarified in Note S1, Supporting Information. Besides, the proposed ES-TENG shows the good capability of energy harvesting along different stimuli directions attributed by the pendulum-like structural design, as illustrated in Figure S6, Supporting Information.

Among various energy sources, wind power is one of the most cost-effective, lowest-priced energy sources available today, which is abundant in the desert, in particular. The ES-TENGs could be hung on the tree branches to harvest the wide distributional wind power in the desert, as shown in Figure 4a. First, the experiments for different wind speed were carried out to measure the output performance of ES-TENG, as demonstrated in Figure 4b. The output of ES-TENG is extremely sensitive to the transient wind, even the light breeze can simulate the efficient electrical output with approximate linear variation. While the wind speed increases over 3 m s^{-1} , the output voltage of the ES-TENG would reach and keep the maximum value ≈ 64 V.

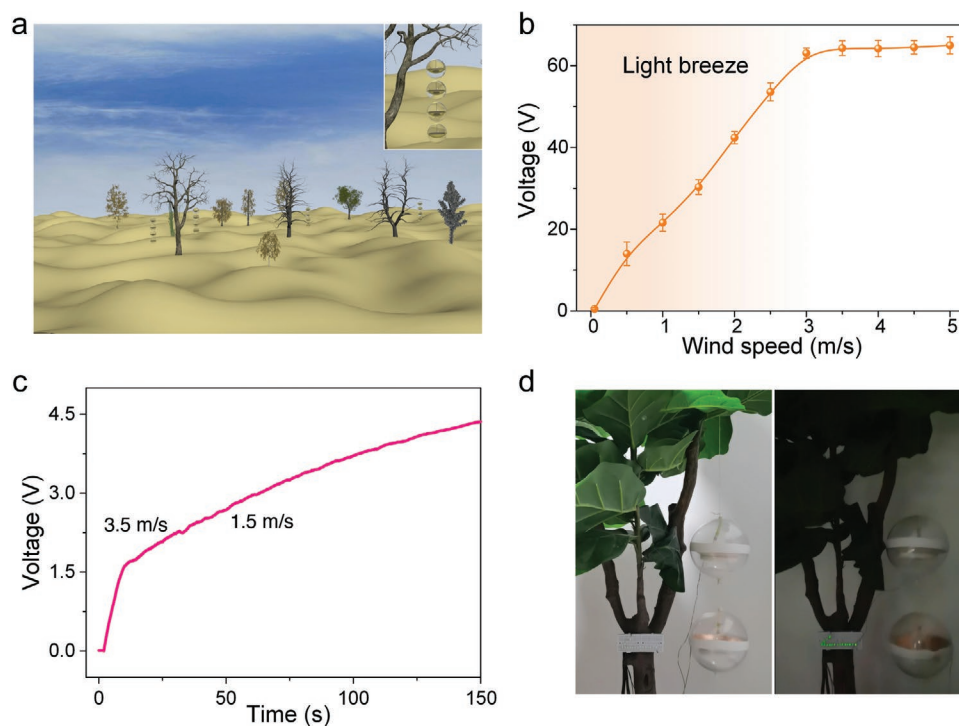


Figure 4. Applications of the ES-TENG for wind energy harvesting. a) Schematic diagram of the ES-TENGs for harvesting the wind energy in the desert. b) Output voltages of the P-TENG with various wind speeds. c) Charging performance of an ES-TENG for a capacitor of 10 μF . d) Photograph of the ES-TENGs to power serial LEDs as the self-powered traffic light.

Figure 4c shows the charging performance of an ES-TENG with the wind speeds of 3.5 and 1.5 m s^{-1} , rendering the ability to harvest wind energy at different situations. Figure 4d demonstrates the ES-TENG to power a series of LEDs as the traffic light, which could be lighted up (Video S1, Supporting Information) and establishing a self-powered traffic indication system.

Water wave energy featuring abundance, wide distribution, and sustainability is deemed to be one of the most prospective clean and renewable power sources for large-scale practical applications, and a schematic diagram of the ES-TENG array for wave energy harvesting is demonstrated in Figure 5a. For achieving efficient energy scavenging and extensive practical applications, a universal power management circuit for the parallel connection is designed and implemented for large scope arrays of the ES-TENGs, as illustrated in Figure 5b in detail. Integrated with the power management circuit, we explored the electrical outputs of the ES-TENG array with different units, as presented in Figure 5c. The peak value of current increases linearly as the elevation of unit number in parallel, but the peak value of voltage keeps remains a constant approximately (Figure S7, Supporting Information), and the output current maximizes at 4.4 μA with six integrated units. Besides, the peak values of voltage for TENGs arranged in series were also experimentally measured, which increase slowly and limited due to the asynchronous output phase, as demonstrated in Figure S8, Supporting Information. Moreover, the charging performance is also investigated, which is consistent with the results of the current in parallel, as depicted in Figure 5d. The capability of energy harvesting for our proposed device compared with the other three designs is

presented in Figure 5e, it can be found that the charging rate is higher than the others. Moreover, the integrated ES-TENG array is successfully applied in water and 80 commercial LEDs could be lighted up by such array continuously, as demonstrated in Figure 5f and Video S2, Supporting Information. Harvesting the wave energy to power distributed sensor nodes is regarded as a promising solution for sustainable, stable, and self-powered information acquisition, wireless transmission, and remote monitoring in the ocean, as the schematic diagram shown in Figure 5g. Here, the self-powered temperature/humidity monitoring system enabled by the integrated ES-TENG array is carried out in the water, as illustrated in Figure 5h,i and Video S3, Supporting Information. The charging and discharging process is displayed in Figure 5h. These applications powerfully prove the outstanding performance of the ES-TENG, greatly accelerating the extensive applications of TENG at a large scale and promoting the self-powered system in IoTs.

3. Conclusions

In summary, an elastic-connection and soft-contact strategy to simultaneously promote the robustness, durability, and efficiency of TENG by introducing an assisted spring and the flexible dielectric fluff with the pendulum-like structural design was proposed, achieving continuous long-term working and multiplied frequency output performance. The pendulum-like structural design assisted by spring can ensure replenished charges consecutively for triboelectrification under the external

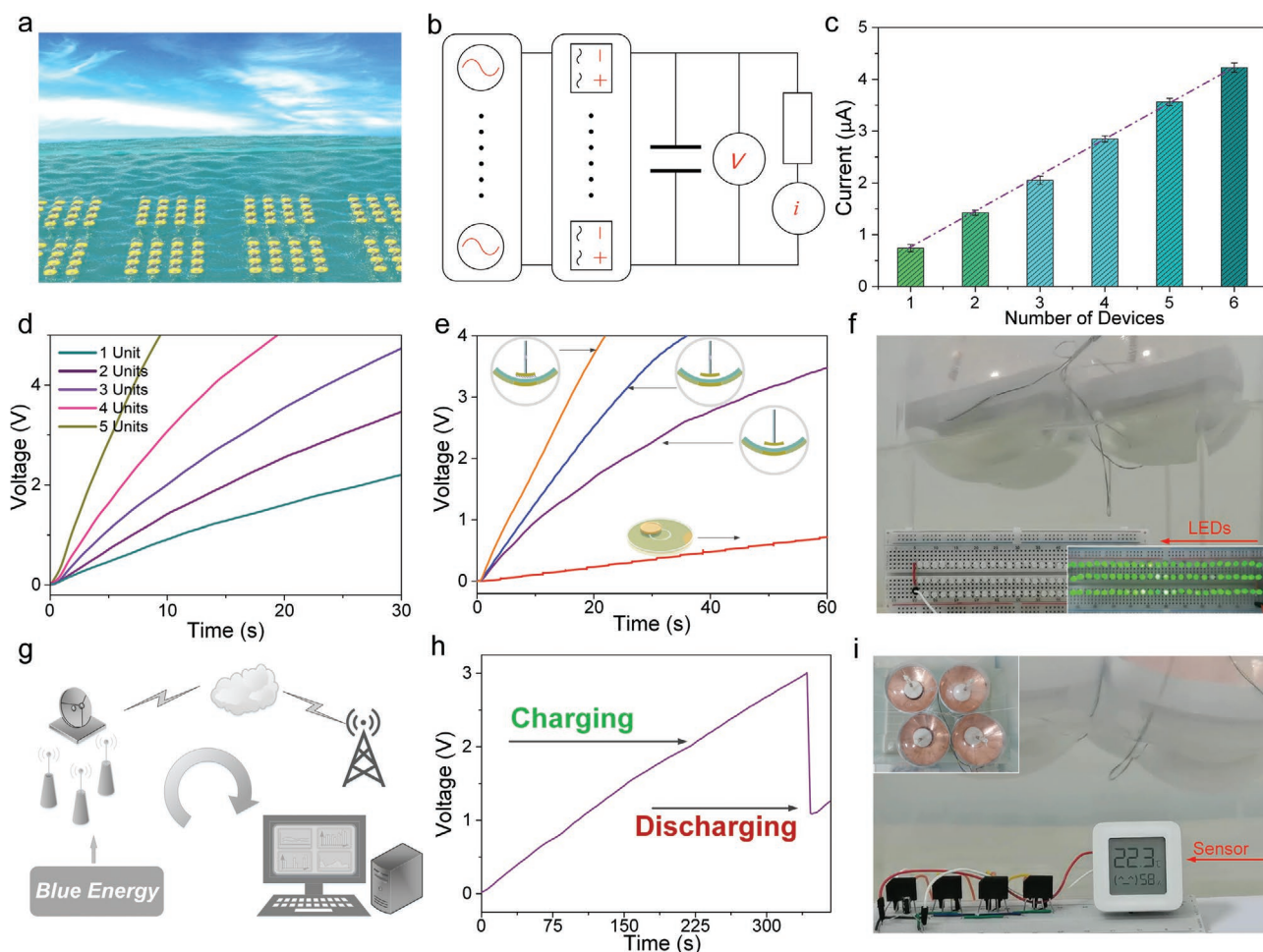


Figure 5. Applications and of the ES-TENG array in water. a) Schematic diagram of ES-TENG array. b) Schematic illustration of the power management circuit. c) Output peak currents of the ES-TENG array with different units. d) Charging performance to a capacitor of 10 μF for different units. e) Comparison of the charging performance for the TENG with different pendulum-like components and conventional in-plane mode structure. f) Photograph of the ES-TENG array to power serial LEDs. g) Imaginary picture of future self-powered information monitoring system in ocean powered by large-scale ES-TENG network. h) Charging and discharging curve of a 47 μF commercial capacitor for the thermometer driven by ES-TENG network. i) Photograph of the ES-TENG network to power a thermometer.

mechanical excitation, leading to frequency-multiplied output and little material abrasion due to the air gap between triboelectric layers. Moreover, the flexible dielectric fluff applied in the design further enhances the triboelectrification for charge accumulation, contributed to the outstanding output performance. Then the output characteristics of the ES-TENG concerning the frequency-multiplied output, charge process, durability, trigger direction, and energy conversion efficiency were systematically studied, proving that the vibration energy-to-electric energy conversion efficiency of 29.7% for one stimulus. Finally, a digital thermometer was successfully driven by the integrated ES-TENG array integrated with the power management circuit, indicating the broad application prospects toward large-scale wave energy scavenging. Given the advantages of exceptional durability and frequency-multiplied output, this research is of great significance to the output and durability of the TENG as well as the applications in large-scale energy harvesting and construction of the self-powered hydrological monitoring system.

4. Experimental Section

Fabrication of the Polymer Nanowires: PTFE film with a thickness of 80 μm was cleaned via acetone and DI water, respectively. Then, a 10 nm thick silver film was deposited on the surface of PTFE film with a deposition rate of 0.5 nm s^{-1} . Finally, the nanowires were obtained by the ICP reactive ion etching with an RF power of 400 W and a bias power of 100 W. The flow rate of the CHF_3 , Ar, and O_2 are controlled into 40, 15, and 10 sccm.

Fabrication of the ES-TENG: The ES-TENG is mainly composed of two major parts: cambered triboelectric layer and pendulum-like sensitive component. The cambered triboelectric layer was tailored by laser cutting (PLS6.75, Universal Laser Systems, USA) based on an acrylic spherical shell with an inner diameter of 130 mm, which was cut as the substrate with a circular diameter of 120 mm. Then a layer of copper (100 nm in thickness) was deposited on a shaped spherical shell through magnetron sputtering with a circular and ring pattern and a layer of PTFE film with a thickness of 80 μm adhered on the surface of the copper layer as the cambered triboelectric layer. The pendulum-like sensitive component was shaped based on the acrylic spherical shell into a cambered acrylic with a circular diameter of 35 mm as the substrate and a layer of flexible dielectric fluff adhered on the surface of it as a triboelectric layer. Then an acrylic rod with a length of 58 mm

was prepared with a spring integrated into the middle as the pendulum rod. The pendulum-like component was connected to the outer acrylic spherical shell (inner diameter: 120 mm) with a cotton thread. The silicone ≈50 g was solidified on the bottom of the inner spherical shell as the mass block. Finally, the acrylic spherical shell was sealed by the sealant to decrease the dielectric shielding effect.

Electric Measurements of the ES-TENG Device: A linear motor (LinMot E1200-P01) was employed to provide the specified external excitation for the ES-TENG oscillation. The open-circuit voltage, short-circuit current, and transferred charge of the ES-TENG were tested by a low-noise preamplifier (Keithley model 6514). A data acquisition system (Model: USB-6218, National Instruments, USA) and a LabVIEW program were conducted to collect the electric data and store it. A water channel controlled by a programmable linear motor was used for the water wave generation.

Supporting Information

Supporting Information is available from the Wiley Online Library or from the author.

Acknowledgements

This research was funded by Fundamental Research Funds for the Central Universities (SWU120045) and Visiting Scholar Foundation of Key Laboratory of Optoelectronic Technology & Systems (Chongqing University), Ministry of Education.

Conflict of Interest

The authors declare no conflict of interest.

Author Contributions

Z.L., B.Z., and Y.X. contributed equally to this work. Z.L. and Z.L.W. conceived the idea, analyzed the data, and wrote the paper. Z.L., B.Z., and Z.L.W. fabricated the ES-TENG and did the electric measurement. Y.X. and J.Y. optimized the structure of the ES-TENG. J.Y. helped with the manuscript. All the authors discussed the results and commented on the manuscript.

Data Availability Statement

Research data are not shared.

Keywords

durability, energy harvesting, frequency multiplied, pendulum-like, triboelectric nanogenerators

Received: June 2, 2021

Revised: June 24, 2021

Published online:

- [1] W. Gao, S. Emaminejad, H. Y. Y. Nyein, S. Challa, K. Chen, A. Peck, H. M. Fahad, H. Ota, H. Shiraki, D. Kiriya, D.-H. Lien, G. A. Brooks, R. W. Davis, A. Javey, *Nature* **2016**, 529, 509.
- [2] X. Pu, H. Guo, J. Chen, X. Wang, Y. Xi, C. Hu, Z. L. Wang, *Sci. Adv.* **2017**, 3, e1700694.
- [3] J. Yang, J. Chen, Y. Su, Q. Jing, Z. Li, F. Yi, X. Wen, Z. Wang, Z. L. Wang, *Adv. Mater.* **2015**, 27, 1316.

- [4] G. Liu, H. Guo, S. Xu, C. Hu, Z. L. Wang, *Adv. Energy Mater.* **2019**, 9, 1900801.
- [5] J. Wang, L. Pan, H. Guo, B. Zhang, R. Zhang, Z. Wu, C. Wu, L. Yang, R. Liao, Z. L. Wang, *Adv. Energy Mater.* **2019**, 9, 1802892.
- [6] W. Deng, Y. Zhou, X. Zhao, S. Zhang, Y. Zou, J. Xu, M.-H. Yeh, H. Guo, J. Chen, *ACS Nano* **2020**, 14, 9050.
- [7] Z. Wen, H. Guo, Y. Zi, M.-H. Yeh, X. Wang, J. Deng, J. Wang, S. Li, C. Hu, L. Zhu, Z. L. Wang, *ACS Nano* **2016**, 10, 6526.
- [8] U. Rajak, F. Khatun, P. Biswas, P. Thakur, *Appl. Phys. Lett.* **2021**, 118, 053502.
- [9] Z. Wu, H. Guo, W. Ding, Y.-C. Wang, L. Zhang, Z. L. Wang, *ACS Nano* **2019**, 13, 2349.
- [10] G. Liu, L. Xiaoa, C. Chen, W. Liu, X. Pu, Z. Wu, C. Hu, Z. L. Wang, *Nano Energy* **2020**, 75, 104975.
- [11] Z. Lin, B. Zhang, H. Guo, Z. Wu, H. Zou, J. Yang, Z. L. Wang, *Nano Energy* **2019**, 64, 103908.
- [12] H. Guo, J. Chen, L. Wang, A. C. Wang, Y. Li, C. An, J.-H. He, C. Hu, V. K. S. Hsiao, Z. L. Wang, *Nat. Sustain.* **2021**, 4, 147.
- [13] H. Guo, M.-H. Yeh, Y. Zi, Z. Wen, J. Chen, G. Liu, C. Hu, H. Guo, Z. L. Wang, *ACS Nano* **2017**, 11, 4475.
- [14] Z. Lin, J. Chen, X. Li, Z. Zhou, K. Meng, W. Wei, J. Yang, Z. L. Wang, *ACS Nano* **2017**, 11, 8830.
- [15] Y. Feng, T. Jiang, X. Liang, J. An, Z. L. Wang, *Appl. Phys. Rev.* **2020**, 7, 021401.
- [16] W. Liu, Z. Wang, G. Wang, G. Liu, J. Chen, X. Pu, Y. Xi, X. Wang, H. Guo, C. Hu, Z. L. Wang, *Nat. Commun.* **2019**, 10, 1426.
- [17] Z. Lin, Y. Wu, Q. He, C. Sun, E. Fan, Z. Zhou, M. Liu, W. Wei, J. Yang, *Nanoscale* **2019**, 11, 6802.
- [18] H. Guo, X. Pu, J. Chen, Y. Meng, M.-H. Yeh, G. Liu, Q. Tang, B. Chen, D. Liu, S. Qi, C. Wu, C. Hu, J. Wang, Z. L. Wang, *Sci. Rob.* **2018**, 3, eaat2516.
- [19] Z. Lin, J. Yang, X. Li, Y. Wu, W. Wei, J. Liu, J. Chen, J. Yang, *Adv. Funct. Mater.* **2018**, 28, 1704112.
- [20] J. Chen, Z. L. Wang, *Joule* **2017**, 1, 480.
- [21] B. Zhang, Z. Wu, Z. Lin, H. Guo, F. Chun, W. Yang, Z. L. Wang, *Mater. Today* **2021**, 43, 37.
- [22] Z. Lin, Z. Wu, B. Zhang, Y.-C. Wang, H. Guo, G. Liu, C. Chen, Y. Chen, J. Yang, Z. L. Wang, *Adv. Mater. Technol.* **2018**, 4, 1800360.
- [23] Y. Chen, Y.-C. Wang, Y. Zhang, H. Zou, Z. Lin, G. Zhang, C. Zou, Z. L. Wang, *Adv. Energy Mater.* **2018**, 8, 1802159.
- [24] S. Zhang, M. Bick, X. Xiao, G. Chen, A. Nashalian, J. Chen, *Matter* **2021**, 4, 845.
- [25] B. Zhang, L. Zhang, W. Deng, L. Jin, F. Chun, H. Pan, B. Gu, H. Zhang, Z. Lv, W. Yang, Z. L. Wang, *ACS Nano* **2017**, 11, 7440.
- [26] Y. Zou, J. Xu, Y. Fang, X. Zhao, Y. Zhou, J. Chen, *Nano Energy* **2021**, 83, 105845.
- [27] B. Zhang, J. Chen, L. Jin, W. Deng, L. Zhang, H. Zhang, M. Zhu, W. Yang, Z. L. Wang, *ACS Nano* **2016**, 10, 6241.
- [28] Y. Zou, A. Libanori, J. Xu, A. Nashalian, J. Chen, *Research* **2020**, 2020, 7158953.
- [29] B. Zhang, G. Tian, D. Xiong, T. Yang, F. Chun, S. Zhong, Z. Lin, W. Li, W. Yang, *Research* **2021**, 2021, 7189376.
- [30] X. Liang, T. Jiang, G. Liu, Y. Feng, C. Zhang, Z. L. Wang, *Energy Environ. Sci.* **2020**, 13, 277.
- [31] Y. Feng, T. Jiang, X. Liang, J. An, Z. L. Wang, *Appl. Phys. Rev.* **2020**, 7, 021401.
- [32] Y. Bai, L. Xua, C. He, L. Zhu, X. Yang, T. Jiang, J. Nie, W. Zhong, Z. L. Wang, *Nano Energy* **2019**, 66, 104117.
- [33] K. Xia, J. Fu, Z. Xu, *Adv. Energy Mater.* **2020**, 10, 2000426.
- [34] Z. Lin, B. Zhang, H. Zou, Z. Wu, H. Guo, Y. Zhang, J. Yang, Z. L. Wang, *Nano Energy* **2020**, 68, 104378.
- [35] T. Jiang, H. Pang, J. An, P. Lu, Y. Feng, X. Liang, W. Zhong, Z. L. Wang, *Adv. Energy Mater.* **2020**, 10, 2000064.